The formation of spiral arms and rings in barred galaxies from the dynamical systems point of view.

Mercè Romero-Gómez

WSIMS 2008
Barcelona

1-5 December 2008

collaborators: J.J. Masdemont, E. Athanassoula

Hubble classification scheme (1925)

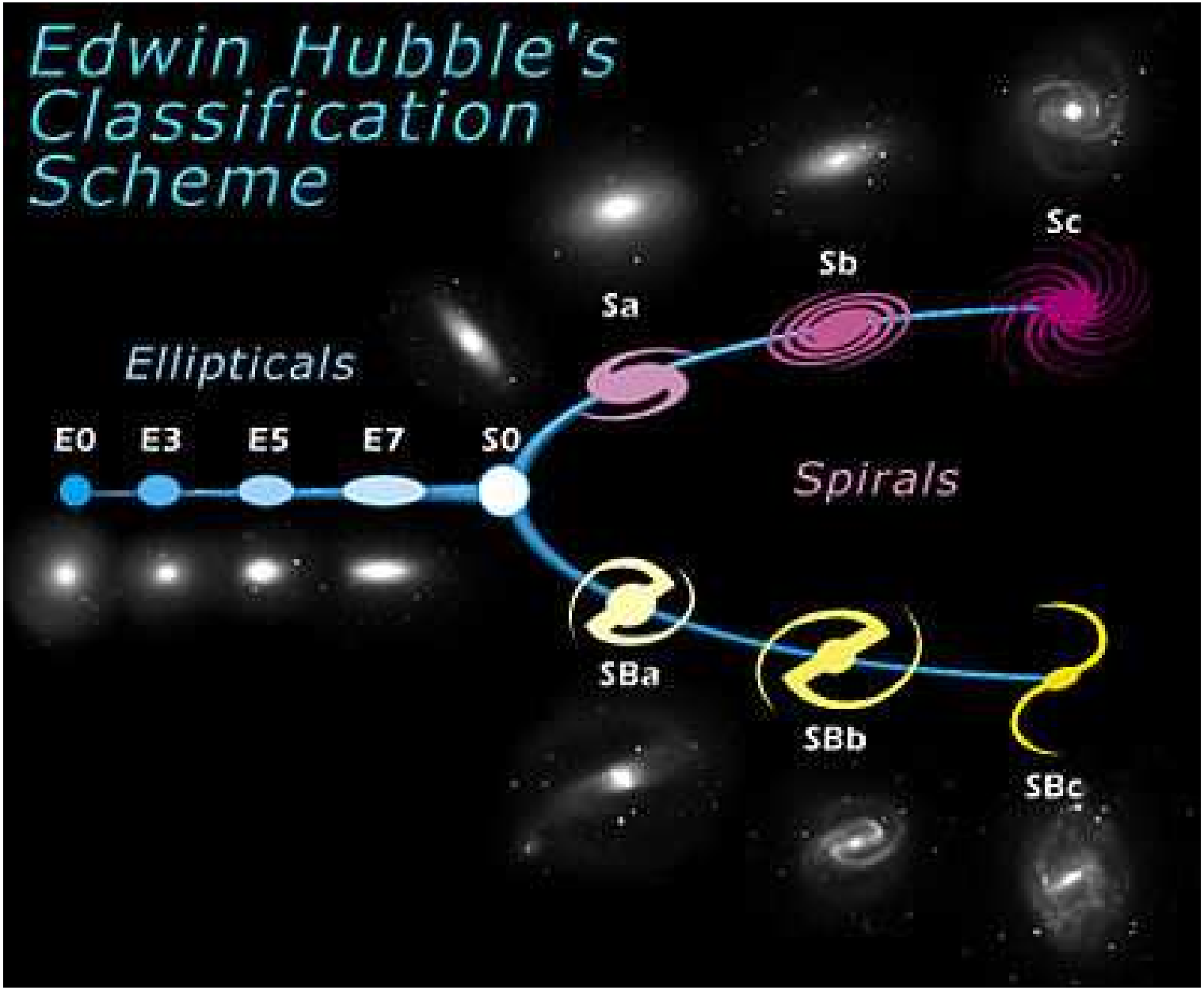

Motivation

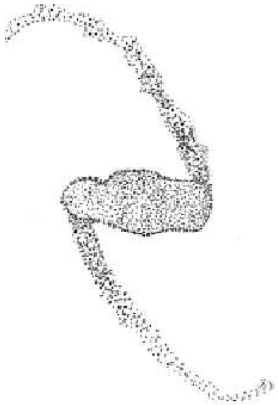
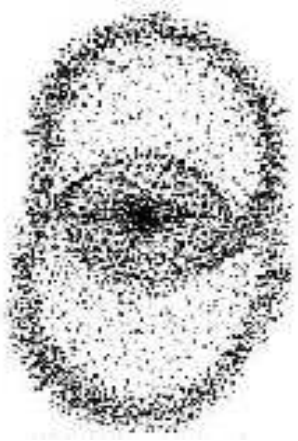
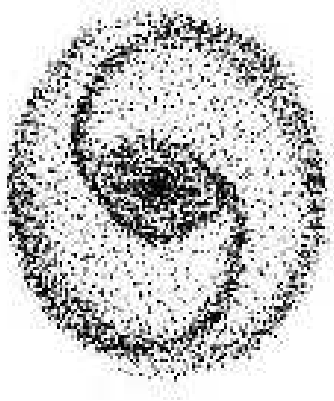
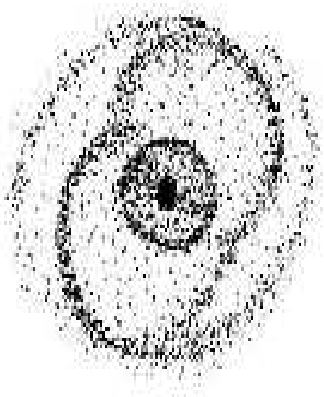


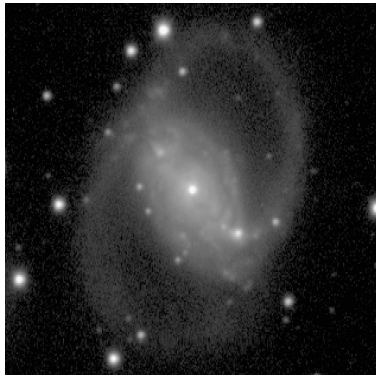
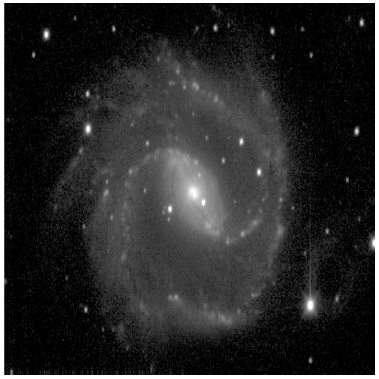
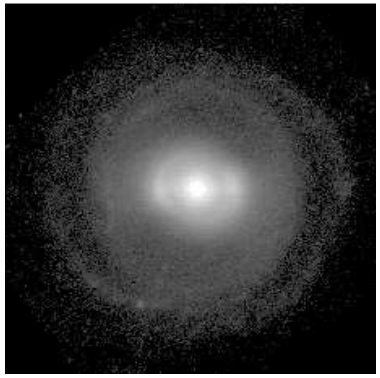

NGC 1365
Spiral arms

NGC 2665
R_1

NGC 2935
R_2

NGC 1079
$R_1 R_2$

Galactic dynamics

- Families of periodic orbits around the central equilibrium point. Main x_1 family gives structure to the bar: Contopoulos, Athanassoula, Pfenniger, Patsis, Petrou, Skokos, Papayannopoulos in the 80s-90s
- Theories on spiral formation, based on the density waves theory: Kalnajs, Lindblad, Lynden-Bell, Lin, Shu, Toomre in the 70s-80s
- N-body simulations: Kohl, Schwarz, Athanassoula, 70s-80s

Basic characteristics of spiral galaxies - I

- Almost all barred galaxies present two spiral arms.
- Early-type spiral galaxies are brighter and more tightly-wound than late-type.
- The sense of winding of the arms with respect to the sense of rotation is mainly trailing.

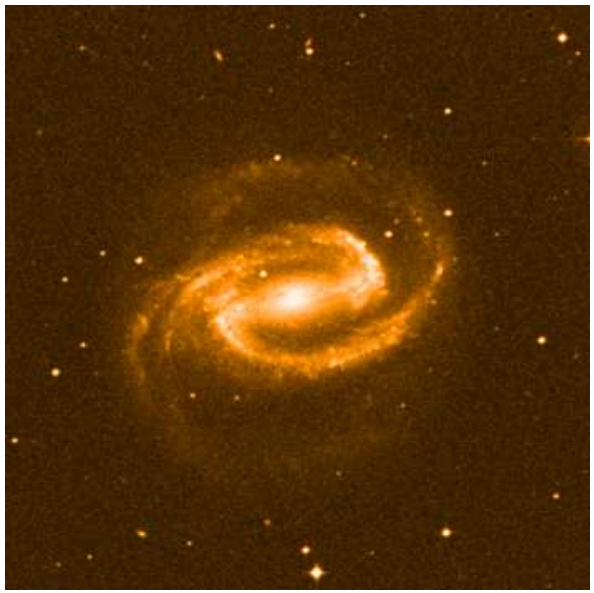

Figure: NGC 1300 - SB(rs)bc

Basic characteristics of spiral galaxies - II Rotation curve

- The rotation curve is the plot of the circular velocity of a hypothetical star as a function of the radius.
- For spiral galaxies, it is typically linearly rising in the central part and flat in the outer region.

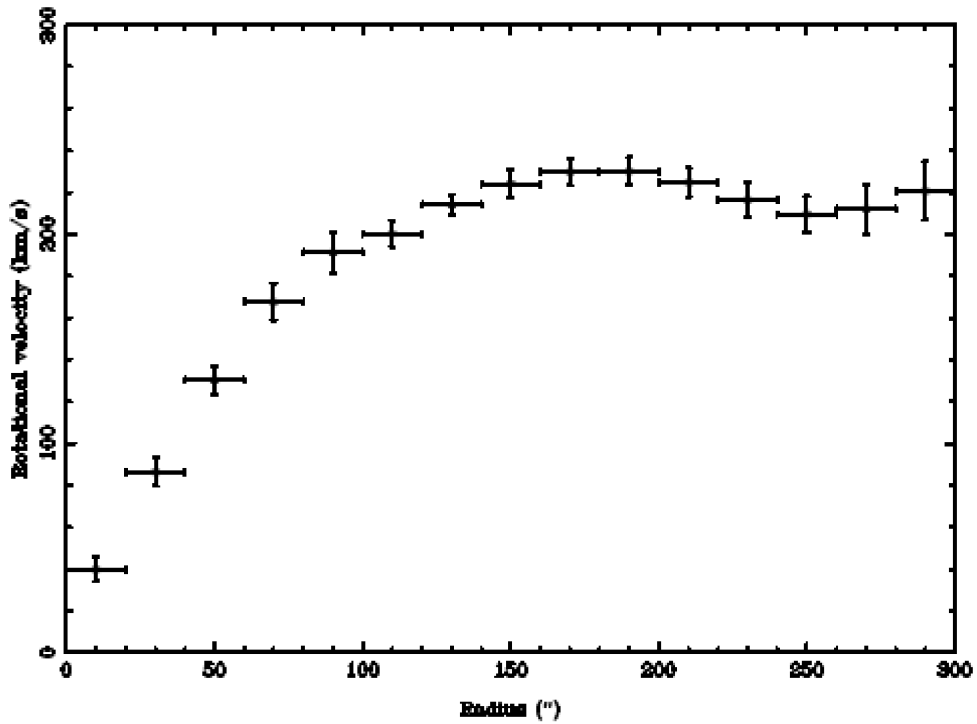

Figure: Rotation curve for NGC 1300; Jörsater, S. and Moorsel, G.A. (1995)

Why studying barred spiral and ringed galaxies? -I

- The origin of spiral structure has been one of the main problems in astrophysics and current theories are kind of "slippery":
  - Swedish astronomer B. Lindblad proposed that spirals result from the gravitational interaction between the orbits of the stars and the disc.
    - Therefore, we have to study them from the stellar dynamics point of view.
    - However, his methods were not appropiate for a quantitative analysis.
  - Lin and Shu proposed that spirals results from a density wave.
    - They can use wave mechanics to explain the properties of the density waves.

Why studying barred spiral and ringed galaxies? -II

- Toomre in the 80s obtains that spirals propagate in the disc from the centre of the galaxy outwards towards one of the principal resonances of the disc, where they damp down:

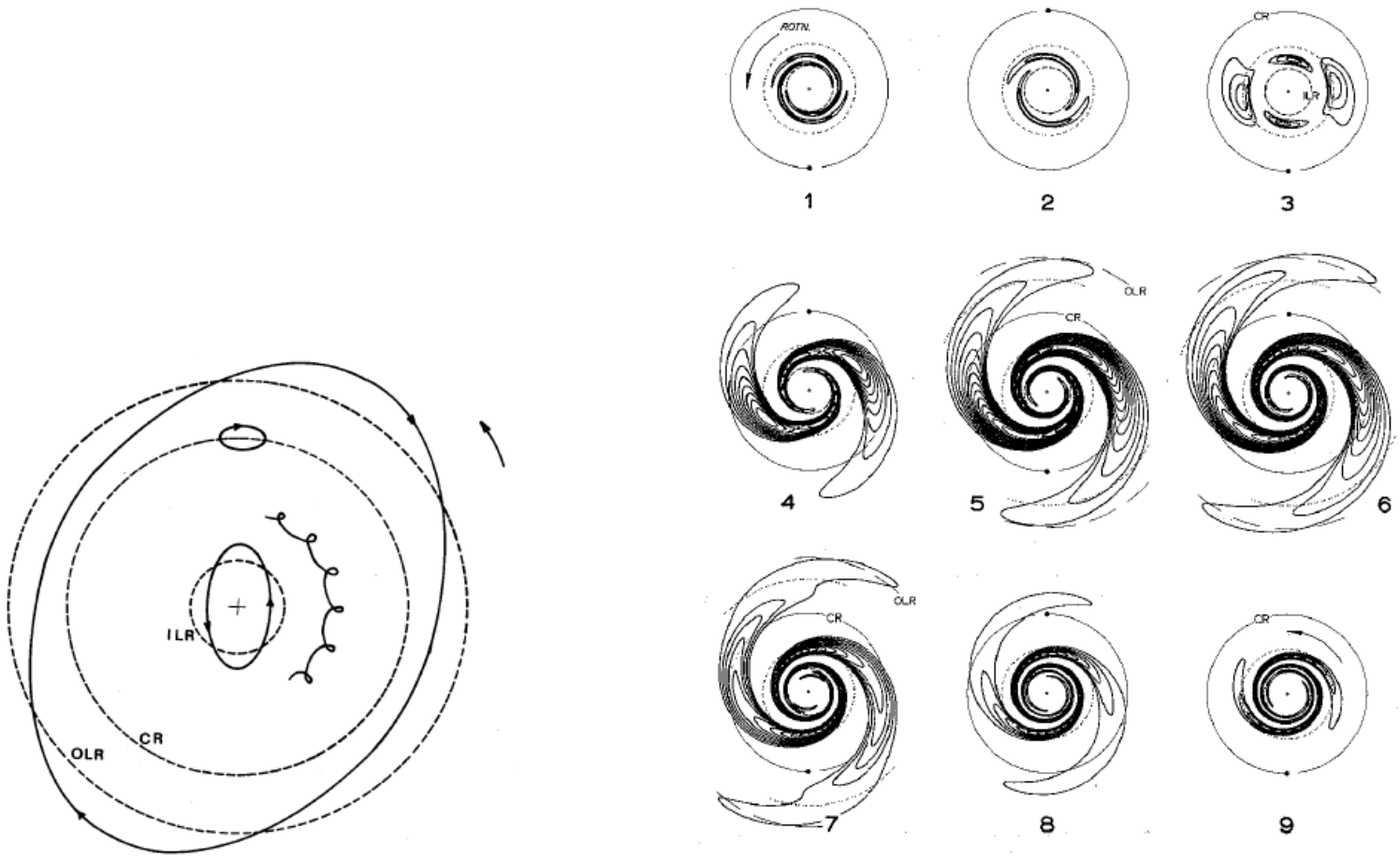

Figure: Toomre (1981)

Obtaining long-lived spirals

Long-lived spirals need replenishment:

- Swing amplification feed-back cycles.
- Driven by a companion.
- Driven by bars.

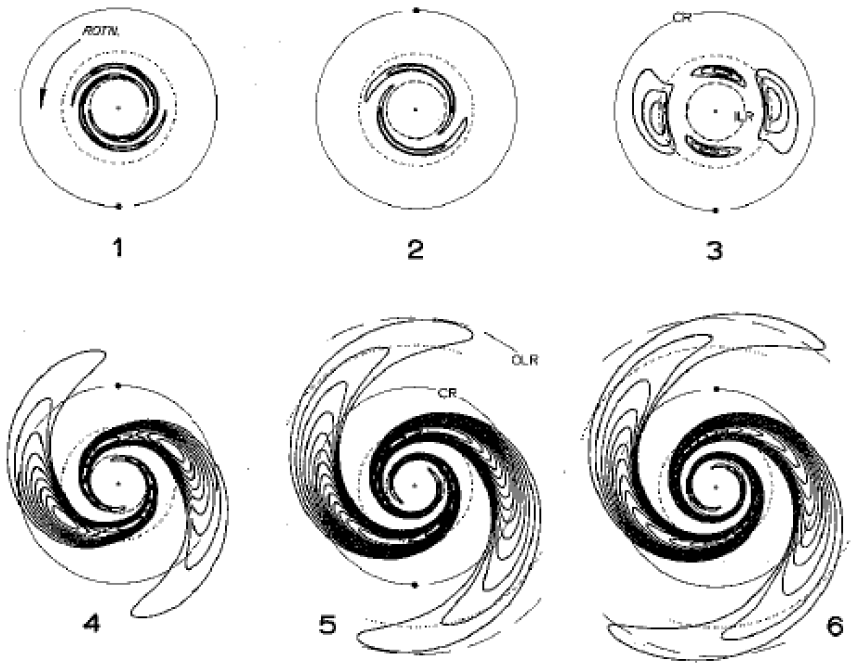

Figure: Toomre (1981)

Kinematic density waves

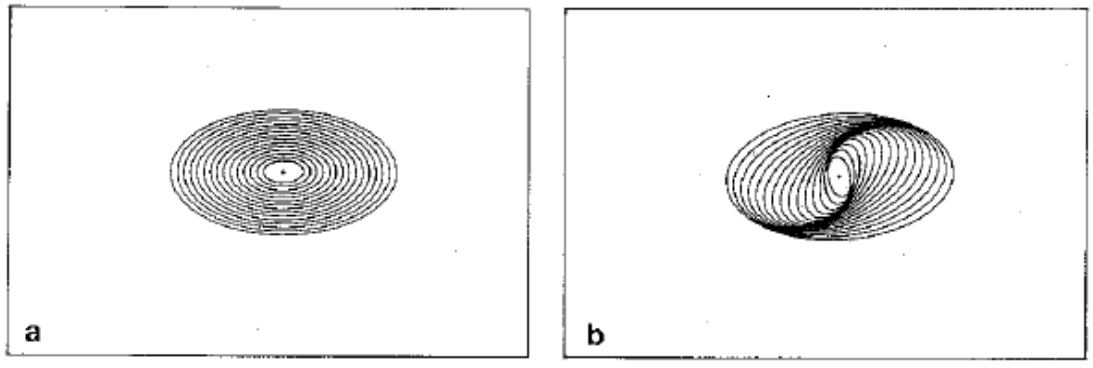

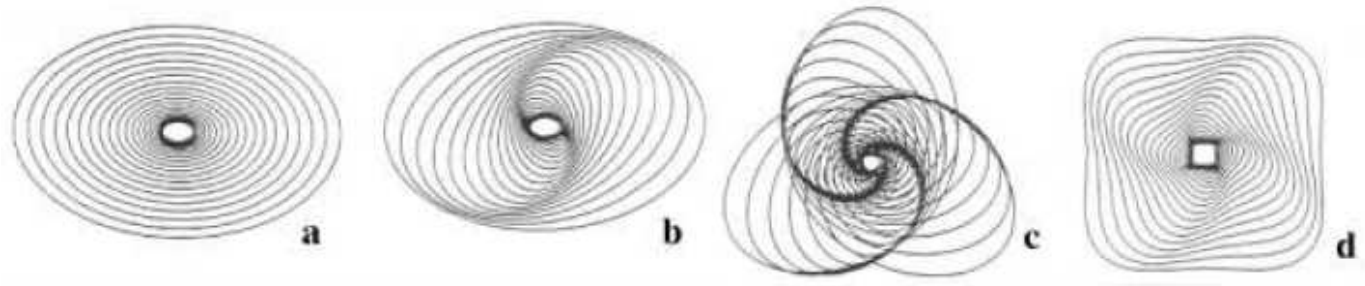

Rings - N-body simulations

Some theories propose that rings are related to the principal resonances of the galaxy:

- ILR related to Nuclear rings
- CR related to Inner rings
- OLR related to Outer rings

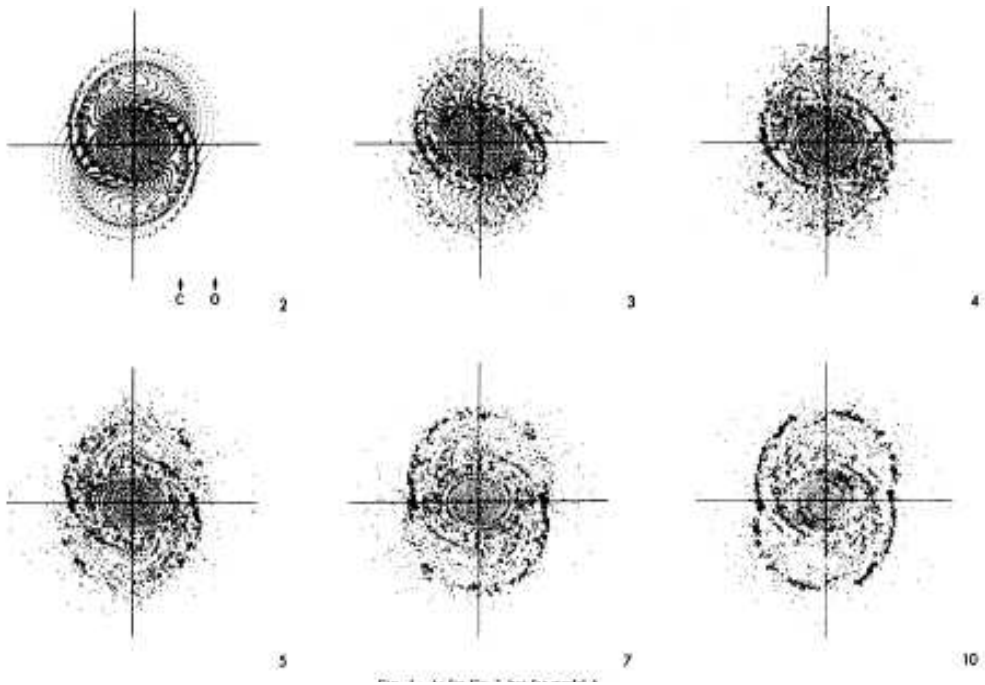

Figure: Schwarz, M.P. (1981)

Components of a barred galaxy

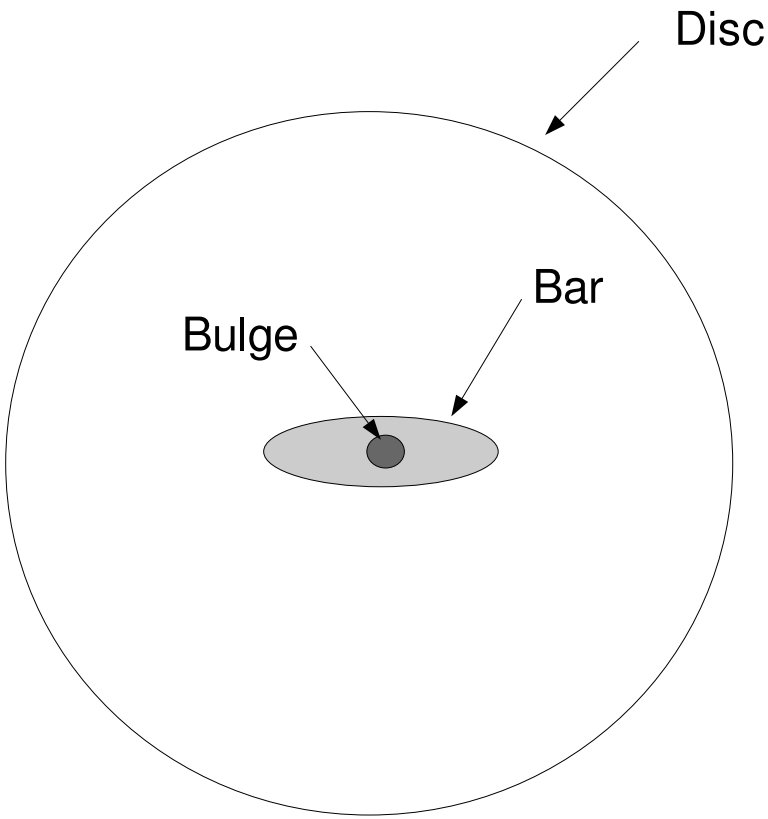

Bar models consist of the superposition of

- Axisymmetric component:
  - a disc: Miyamoto-Nagai, Kuzmin/Toomre potentials.
  - a spheroid or bulge: Plummer, spherical potentials.
- and a bar: Ferrers ellipsoids, ad-hoc bar potentials.

The disc

- Discs are flattened, roughly axisymmetric, disc-like structures.
- They have an exponential surface-brightness distribution.
- Represented by Miyamoto-Nagai or Kuzmin/Toomre disc potentials.

$$\Phi_M(R) = -\frac{GM}{\sqrt{R^2 + A^2}}$$

$$\Phi_K(R) = -\frac{3}{2}V_0^2 \left(\frac{3/2}{1/2 + R^2/r_0^2} \right)^{1/2}$$

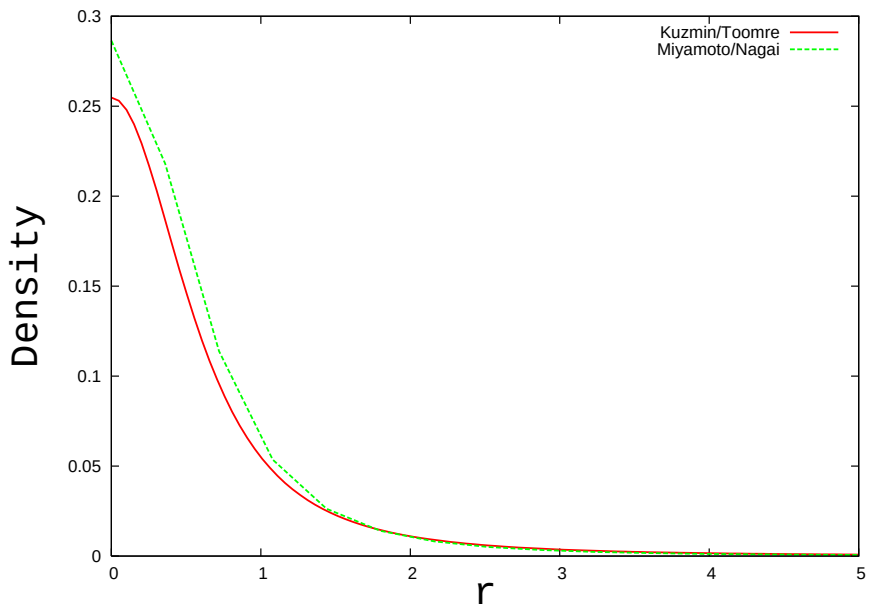

The spheroid/halo

- They are roughly spherical distributions of stars.
- Represented by a Plummer spheroid or any spheric density distribution.

$$\rho_P(R) = \left(\frac{3M}{4\pi B^3}\right)\left(1+\frac{R^2}{B^2}\right)^{-5/2}$$

$$\rho(R) = \rho_b\left(1+\frac{R^2}{r_b^2}\right)^{-3/2}$$

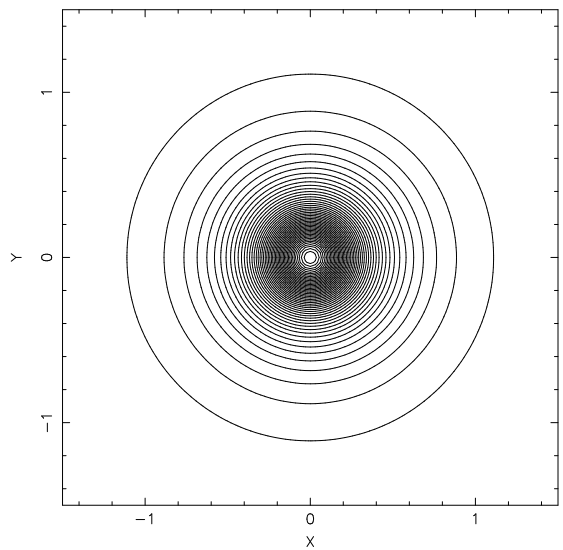

Figure: Isodensity curves for the spheroid.

Bar characteristics

- Bars are non-axisymmetric triaxial features with high ellipticities. The typical axes have length scales proportional to 1:2.
- Bars are not centrally condensed. The surface brightness is
  - nearly constant along the semi-major axis.
  - steep and falls off sharply along the semi-minor axis.
- Bars extend up to CR. The ratio $R_{CR}/a = 1.2 \pm 0.2$ and rotate (Athanassoula 1992)

Bar component

- Ferrer's ellipsoid: $\rho = \begin{cases} \rho_0(1-m^2)^n & m \leq 1 \\ 0 & m \geq 1, \end{cases}$

  $\Phi(x,y,z) =$

  $$-\pi G a b c \rho_0 \sum_{i+j+k+l=n+1} \frac{n!}{i!j!k!l!}(-1)^{n-i} x^{2j} y^{2k} z^{2l} W_{jkl}$$

- Logarithmic type: $\Phi(x,y,z) = \frac{1}{2}\nu_0^2 \log\left(R_0^2 + x^2 + \frac{y^2}{p^2} + \frac{z^2}{q^2}\right)$

- Dehnen's bar type:

  $$\Phi(r,\theta) = -\tfrac{1}{2}\epsilon v_0^2 \cos(2\theta) \begin{cases} 2 - \left(\frac{r}{a}\right)^n & , \quad r \leq a \\ \left(\frac{a}{r}\right)^n & , \quad r \geq a \end{cases}$$

- Barbanis-Woltjer's type: $\Phi(r,\theta) = \hat{\epsilon}\sqrt{r}(r_1 - r)\cos(2\theta)$

Equations of motion

- The equations of motion of a rotating system are described in vectorial form by:

$$\ddot{\mathbf{r}} = -\nabla \mathbf{\Phi}_{\text{eff}} - 2(\mathbf{\Omega} \times \dot{\mathbf{r}}),$$

  where $\mathbf{r} = (x, y, z)$ is the position vector and $\mathbf{\Omega} = (0, 0, \Omega)$ is the rotation velocity vector around the z-axis, and $\Phi_{\text{eff}} = \Phi - \frac{1}{2}\Omega^2 (x^2 + y^2)$ is the effective potential.
- We define the Jacobi constant or Jacobi energy as $E_J = \frac{1}{2}|\dot{\mathbf{r}}|^2 + \Phi_{\text{eff}}$.
- The zero velocity surface of a given energy level is the surface obtaine when: $\Phi_{\text{eff}}(x, y, z) = E_J$. We define the zero velocity curve, its cut with the $z = 0$ plane.

Equilibrium points

- The equilibrium points of the system are located where

$$\frac{\partial \Phi_{\text{eff}}}{\partial x} = \frac{\partial \Phi_{\text{eff}}}{\partial y} = \frac{\partial \Phi_{\text{eff}}}{\partial z} = 0.$$

They lie on the xy-plane: L_1 and L_2 along the bar major axis, L_3 on the origin, and L_4 and L_5 along the bar minor axis.

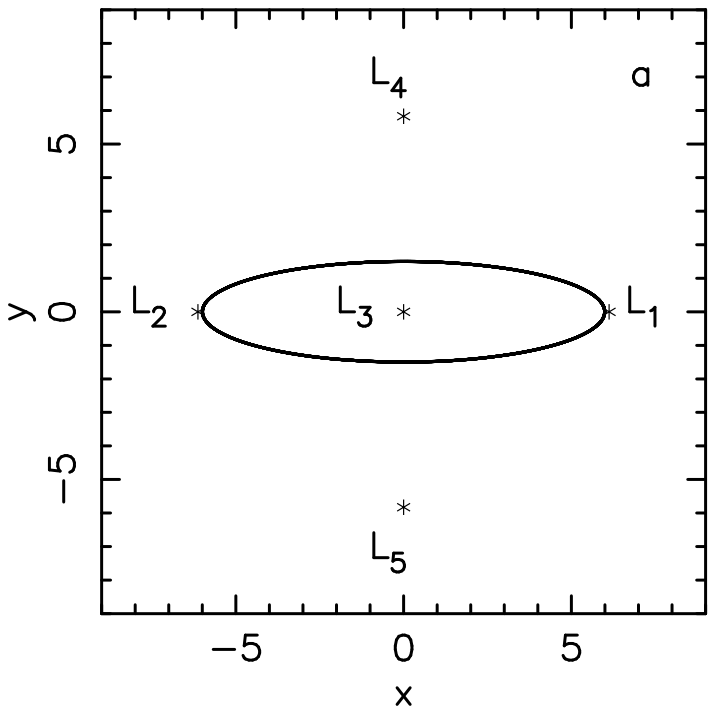

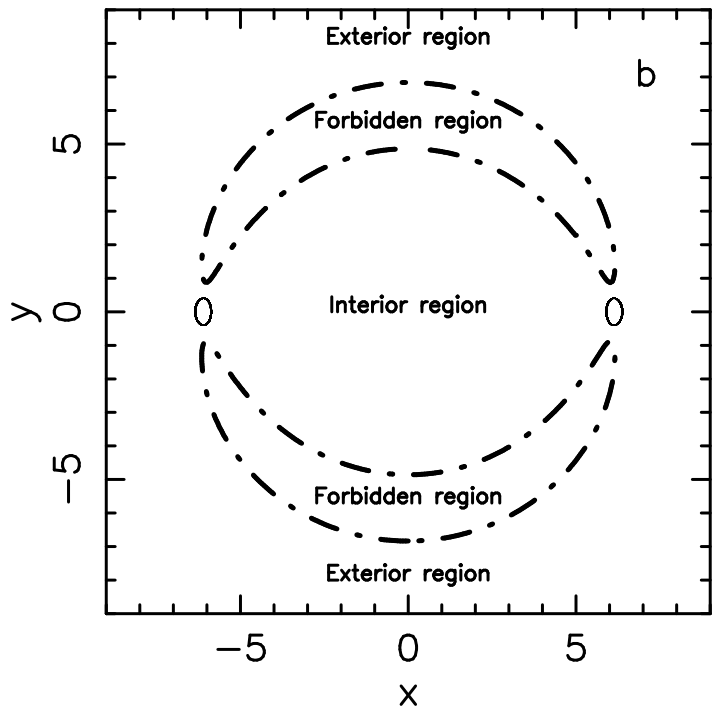

Lyapunov orbits

- We focus on the motion around the hyperbolic points L_1 and L_2
- The linear motion around $L_1(L_2)$ has the expression:

$$\begin{cases} x(t) = X_1 e^{\lambda t} + X_2 e^{-\lambda t} + X_3 \cos(\omega t + \phi), \\ y(t) = A_1 X_1 e^{\lambda t} - A_1 X_2 e^{-\lambda t} + A_2 X_3 \sin(\omega t + \phi), \\ z(t) = X_7 \cos(\nu t + \psi). \end{cases}$$

- On the xy-plane and integrating an initial condition obtained from setting $X_1 = X_2 = 0$, we obtained the periodic motion $\mathbf{x}_0(t) = (x(t), y(t), \dot{x}(t), \dot{y}(t))$

$$\mathbf{x}_0(t) = (X_3 \cos(\omega t+\phi), A_2 X_3 \sin(\omega t+\phi), -X_3\omega \sin(\omega t+\phi), A_2 X_3 \omega \cos(\omega t+\phi))$$

We refer to it as the linear planar Lyapunov periodic orbit.

Linear Invariant manifolds associated to periodic orbits

- The linear stable and unstable invariant manifolds are obtained from integrating initial conditions with $X_1 = 0$ and $X_2 \neq 0$, and $X_1 \neq 0$ and $X_2 = 0$, respectively.

$$\begin{cases} x(t) = X_1 e^{\lambda t} + X_2 e^{-\lambda t} + X_3 \cos(\omega t + \phi), \\ y(t) = A_1 X_1 e^{\lambda t} - A_1 X_2 e^{-\lambda t} + A_2 X_3 \sin(\omega t + \phi). \end{cases}$$

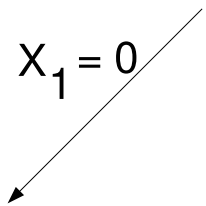

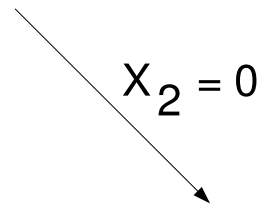

$$\begin{cases} x(t) = X_2 e^{-\lambda t} + X_3 \cos(\omega t + \phi), \\ y(t) = -A_1 X_2 e^{-\lambda t} + A_2 X_3 \sin(\omega t + \phi). \end{cases}$$

Linear Stable Invariant Manifold

$$\begin{cases} x(t) = X_1 e^{\lambda t} + X_3 \cos(\omega t + \phi), \\ y(t) = A_1 X_1 e^{\lambda t} + A_2 X_3 \sin(\omega t + \phi). \end{cases}$$

Linear Unstable Invariant Manifold

Nonlinear stable and unstable invariant manifolds

- Using NF - reduction to the centre manifold
- "Directly", integrating i.c. taken in the direction given by the most unstable eigenvalue of the monodromy matrix.

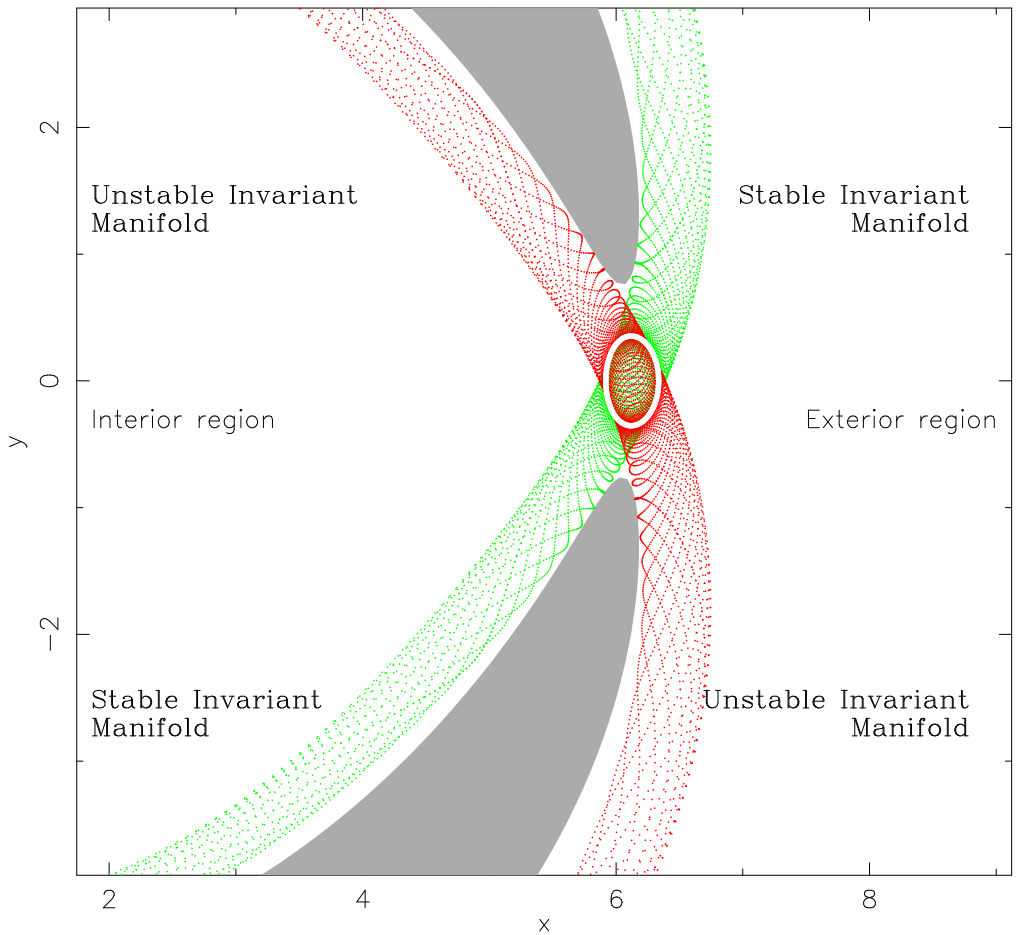

Romero-Gómez et al. (2006)

Transit orbits

Transfer of matter from the interior to the exterior region:

- Transit orbits have initial conditions *inside* the $W^{s,1}_{\gamma_i}$ curve in the $y\dot{y}$ plane.
- Non-transit orbits have initial conditions *outside* the $W^{s,1}_{\gamma_i}$ curve in the $y\dot{y}$ plane.

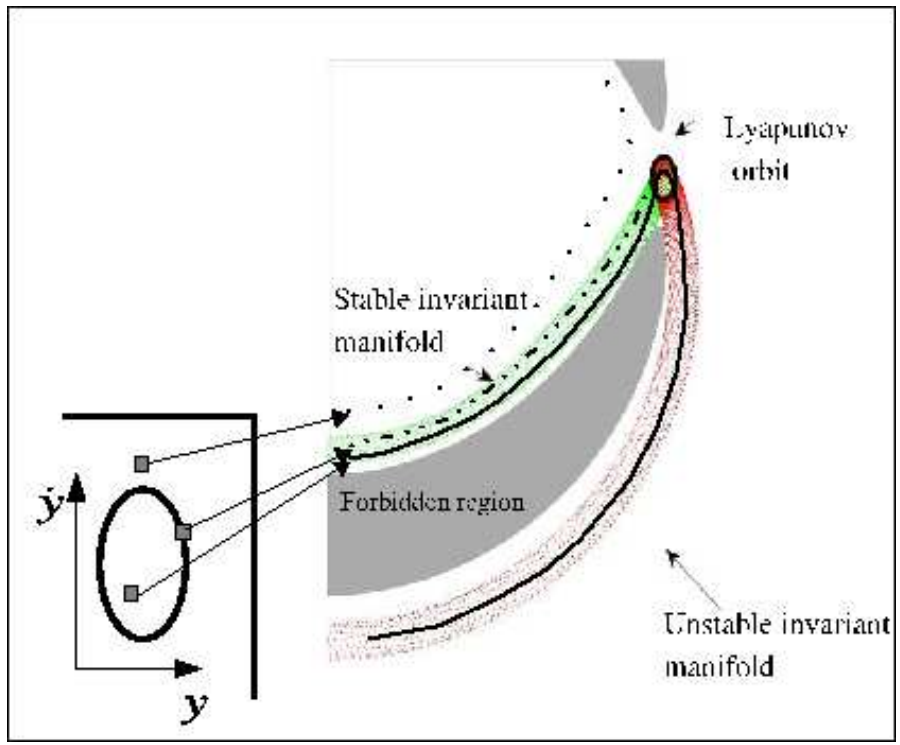

Transfer of matter: Homoclinic and heteroclinic orbits

- Homoclinic orbits, ψ, s.t. $\psi \in W^u_{\gamma_i} \cap W^s_{\gamma_i}$, $i = 1, 2$
- Heteroclinic orbits, ψ', s.t. $\psi' \in W^u_{\gamma_i} \cap W^s_{\gamma_j}$, $i \neq j$, $i, j = 1, 2$

Romero-Gómez et al. (2007)

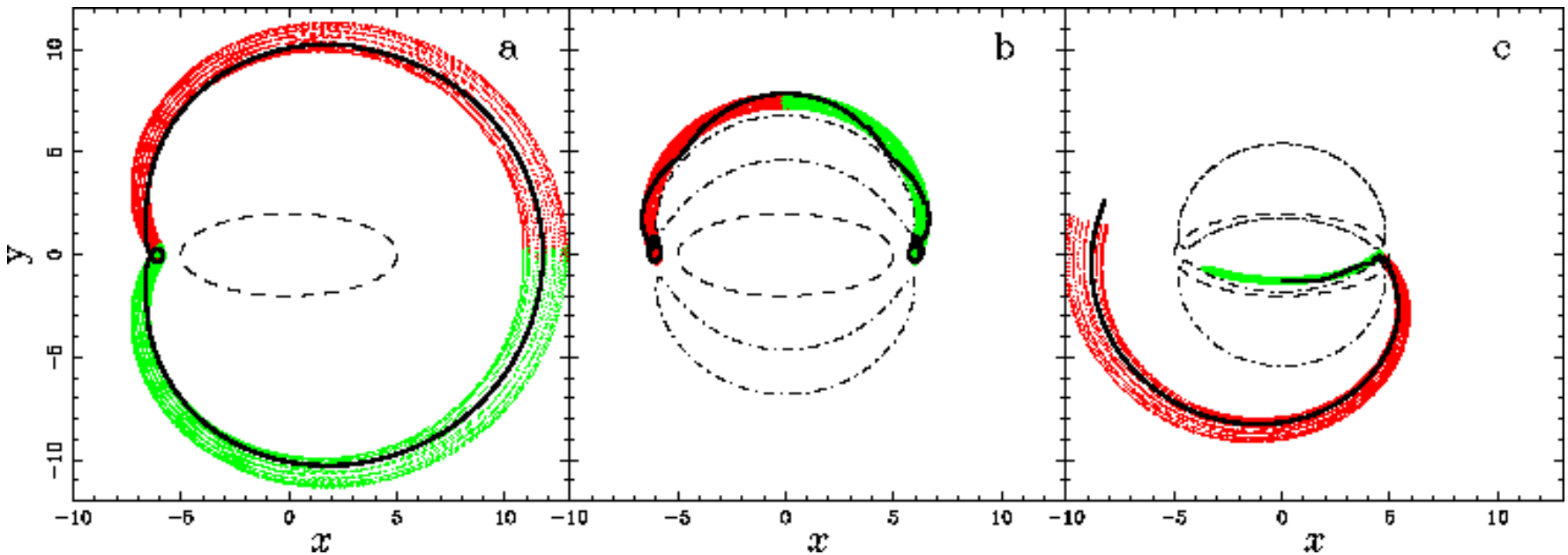

Homoclinic Heteroclinic Transit

Motivation

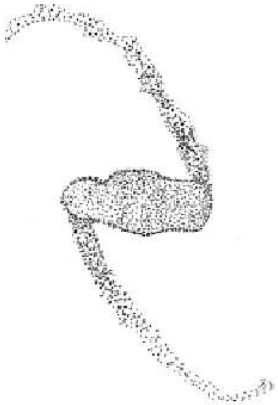
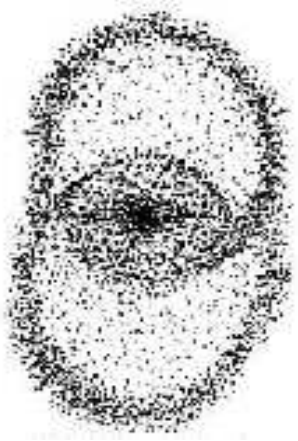
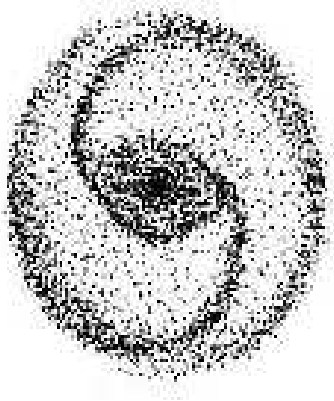
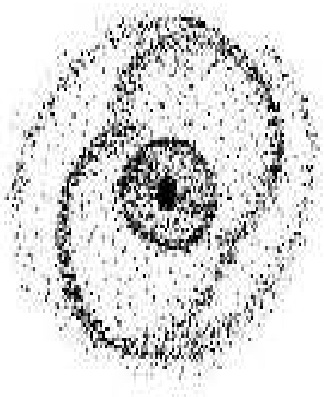


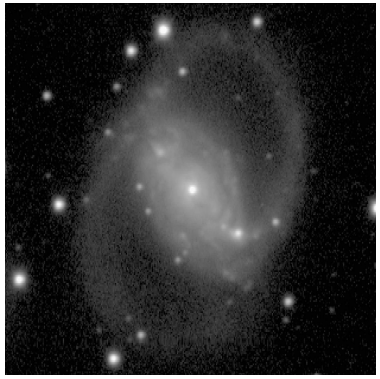
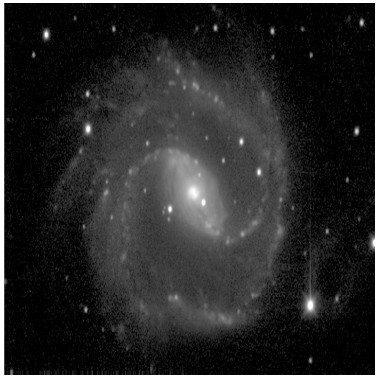
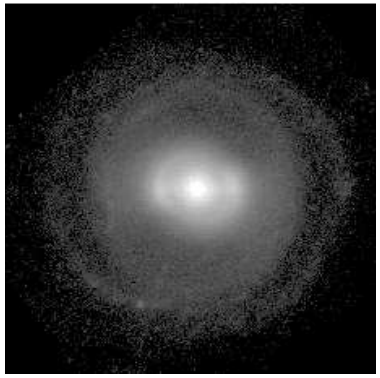

NGC 1365
Spiral arms

NGC 2665
R_1

NGC 2935
R_2

NGC 1079
$R_1 R_2$

R_1 rings

- If there exist heteroclinic orbits, the morphology obtained is **rR$_1$ ring** structure.

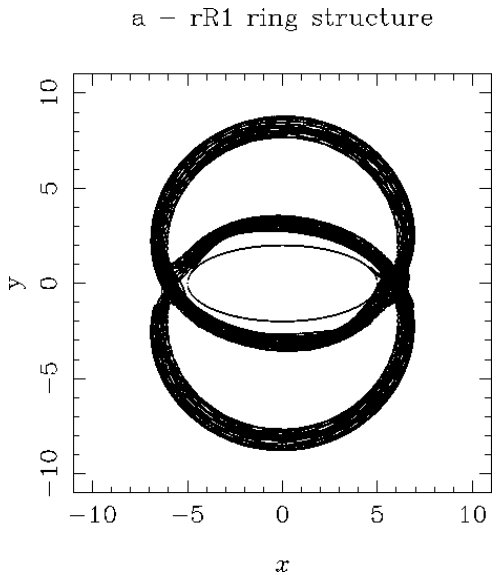

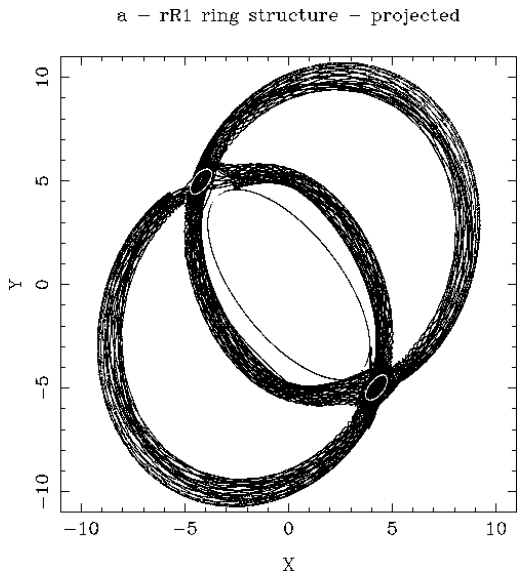

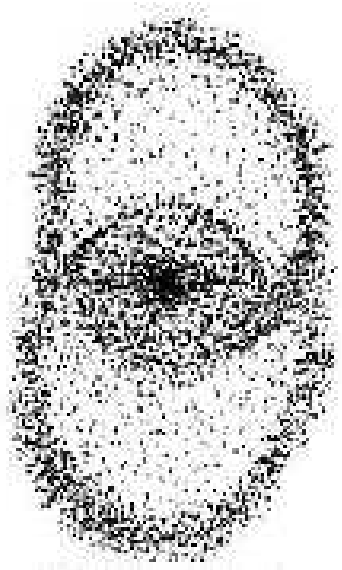

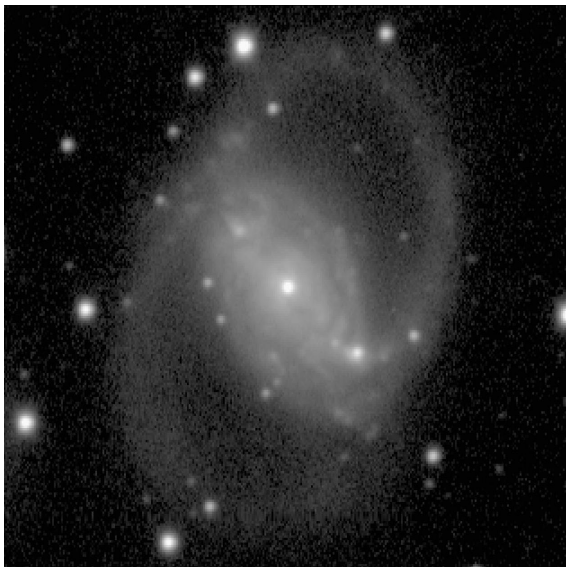

R_1R_2 rings

- If there exist homoclinic orbits, the morphology obtained is **rR$_1$R$_2$ ring** structure.

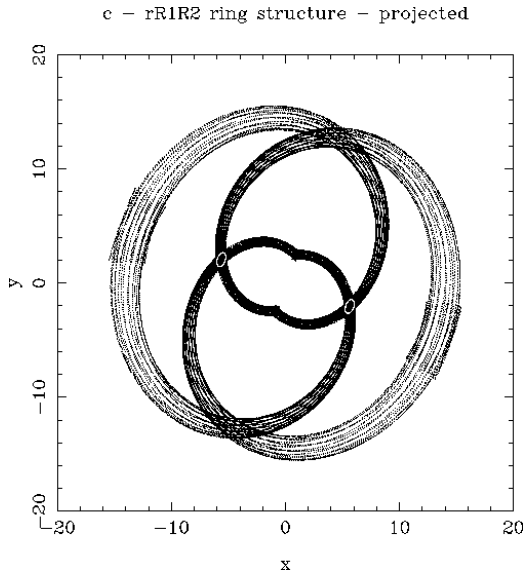

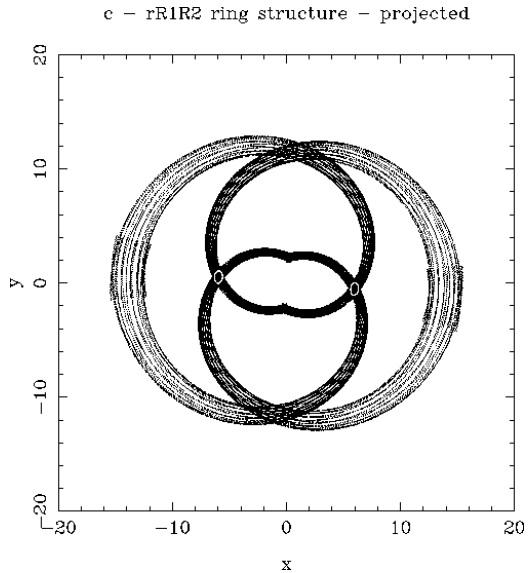

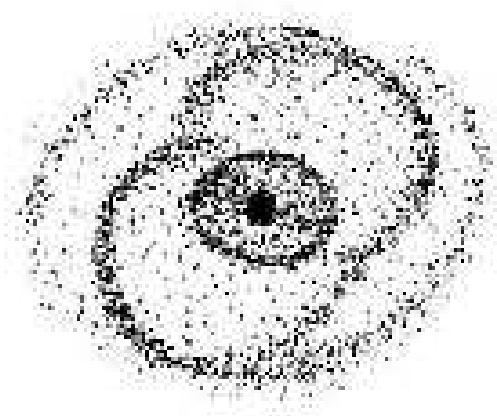

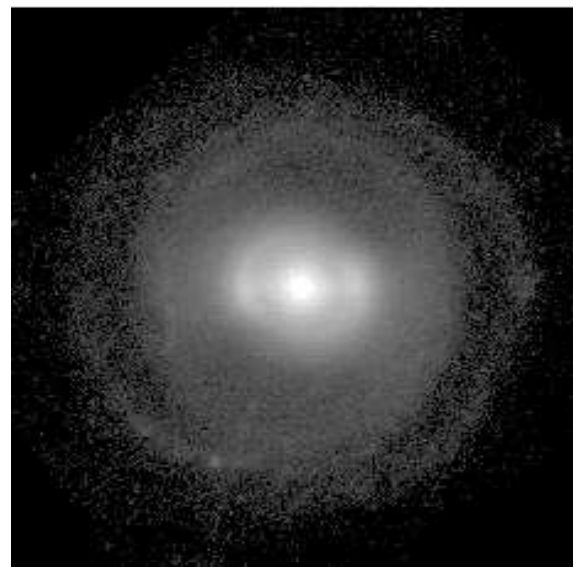

Spiral arms

- If there are no heteroclinic or homoclinic orbits, the morphology obtained is two **spiral arms**.

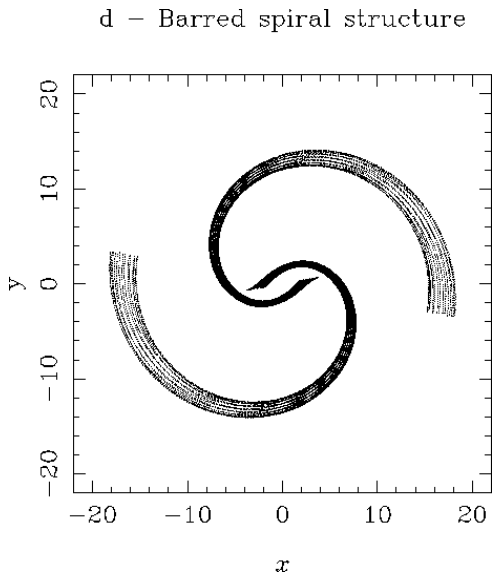

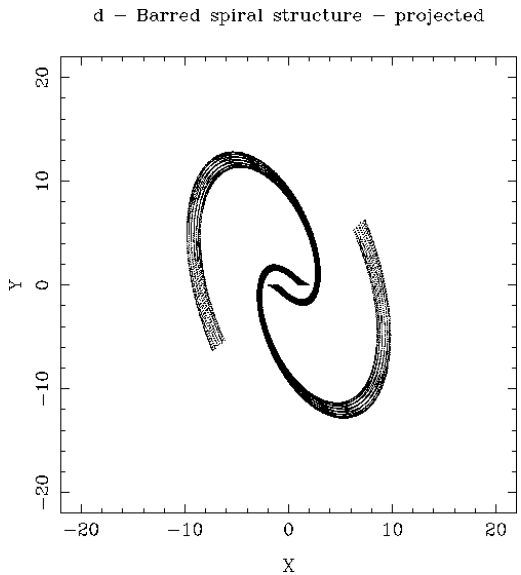

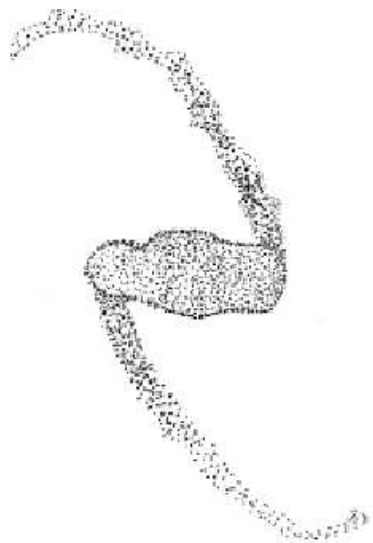

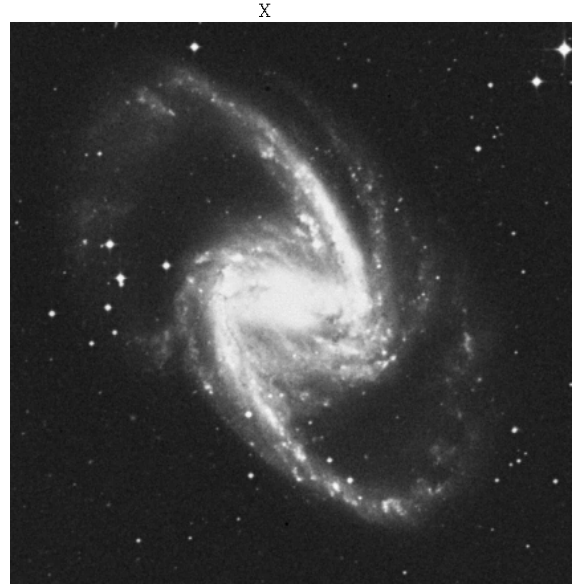

R_2 rings

- When the pitch angle is adequate, the spiral arms cross each other and form **R_2 rings**.

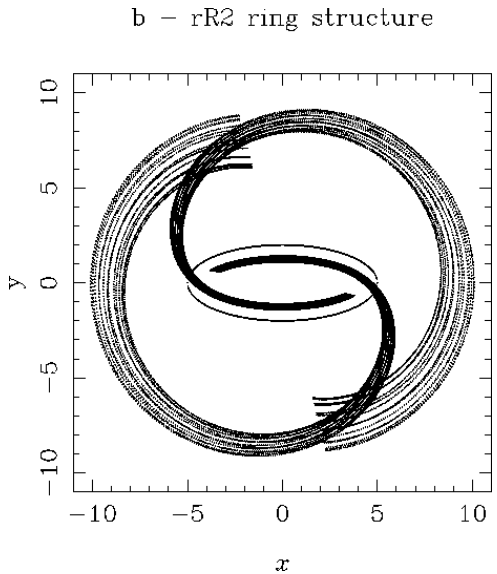

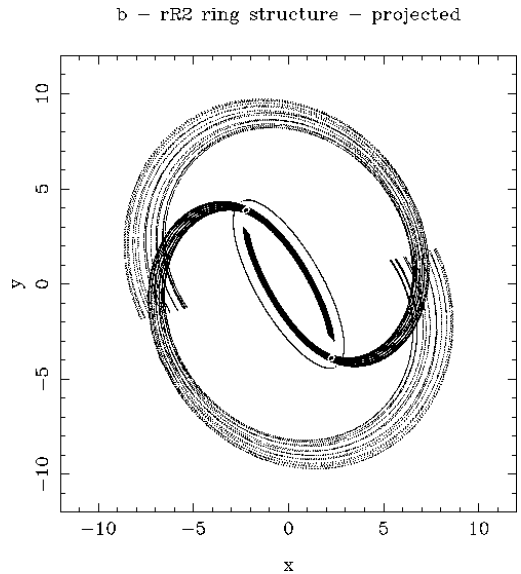

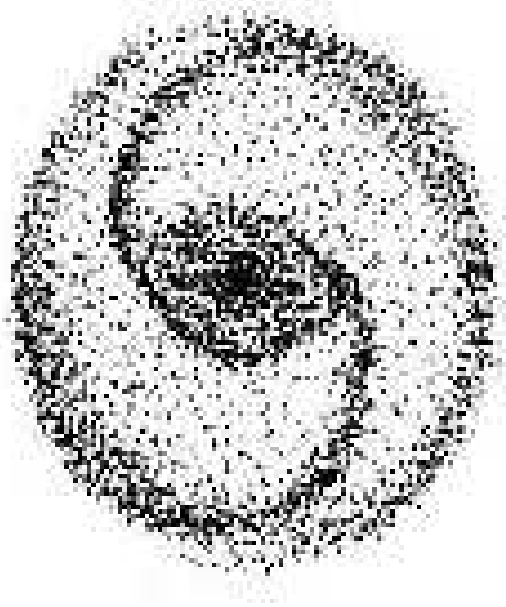

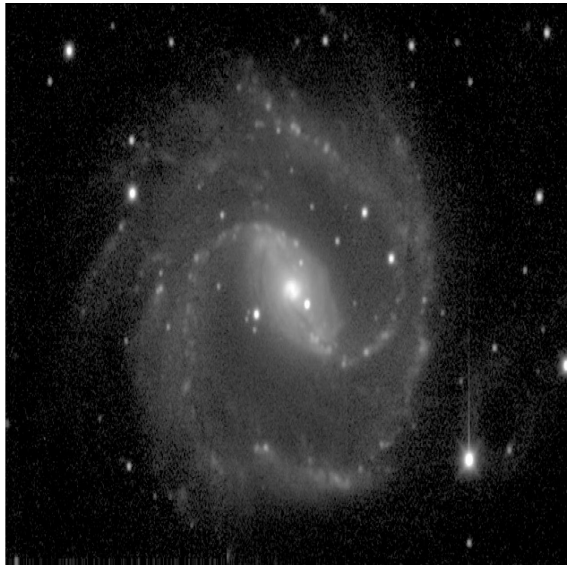

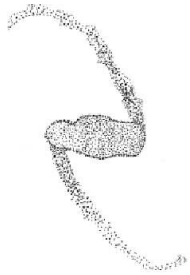

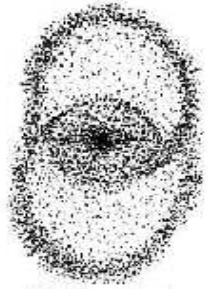

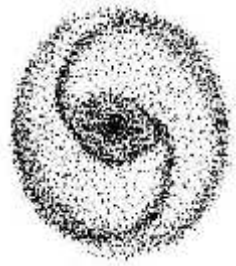

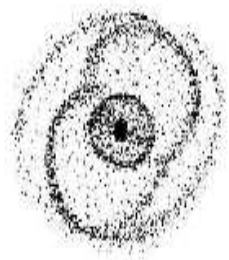

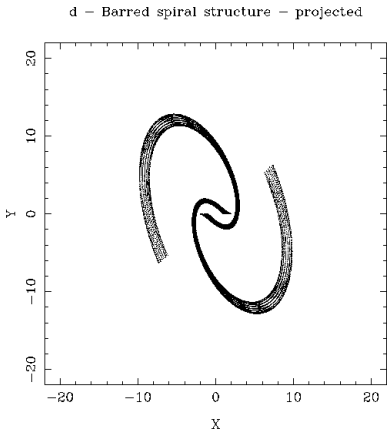

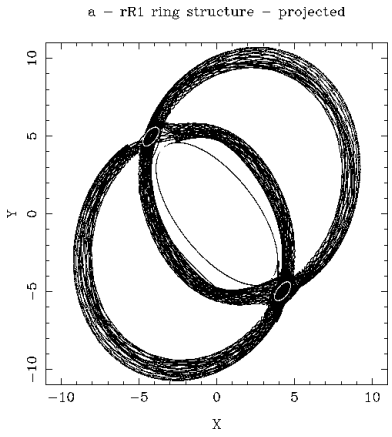

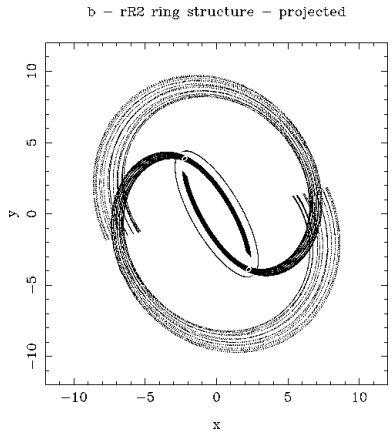

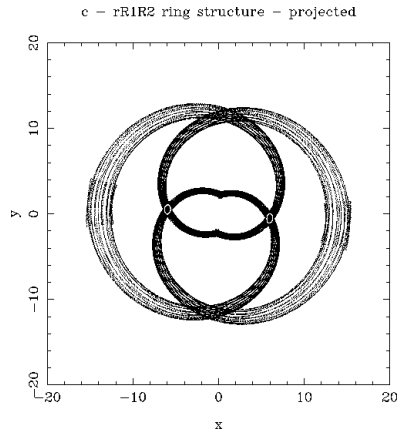

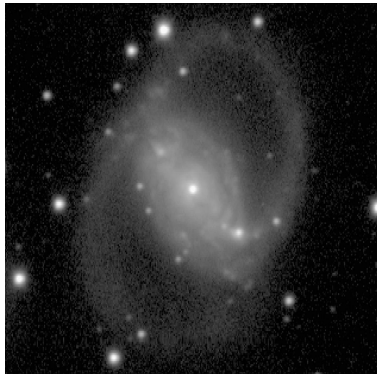

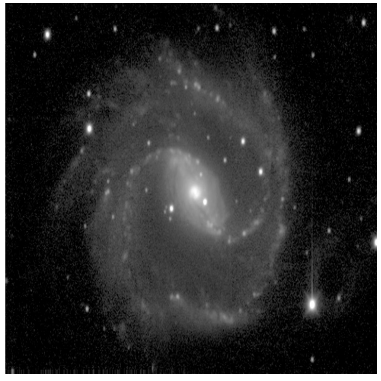

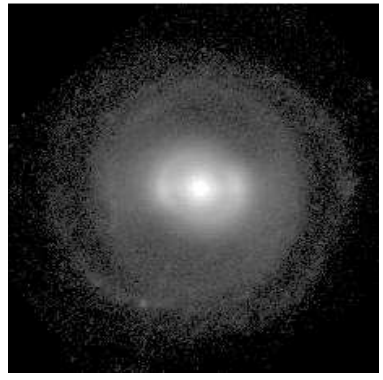

NGC 1365
Spiral arms

NGC 2665
R_1

NGC 2935
R_2

NGC 1079
R_1R_2

Simulation - response. Where does all the material on these orbits comes from? Only from the immediate neighbourhood of the Lagrangian points?

Not necessarily. In fact, most of it can come from the outer parts of the bar, driven to the L_1/L_2 and to the unstable manifold by the inner branch of the stable manifold.

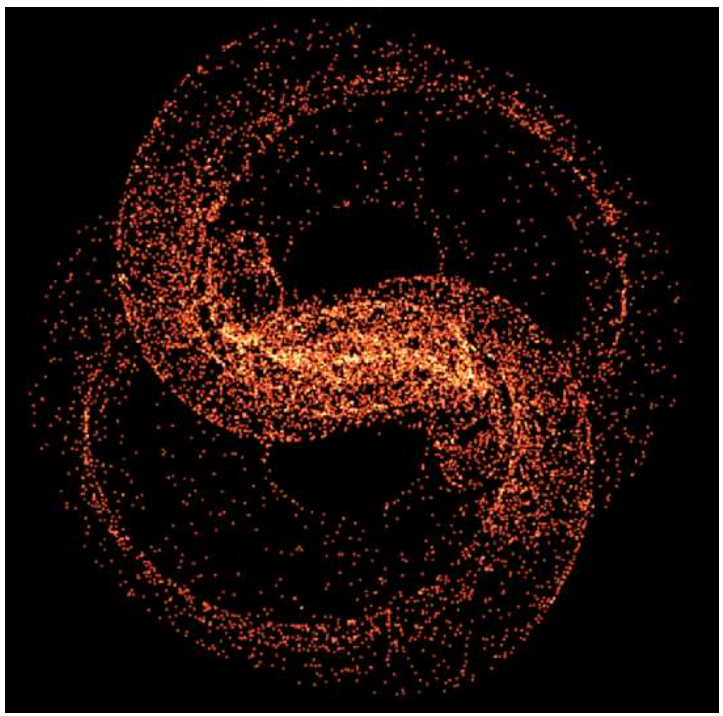

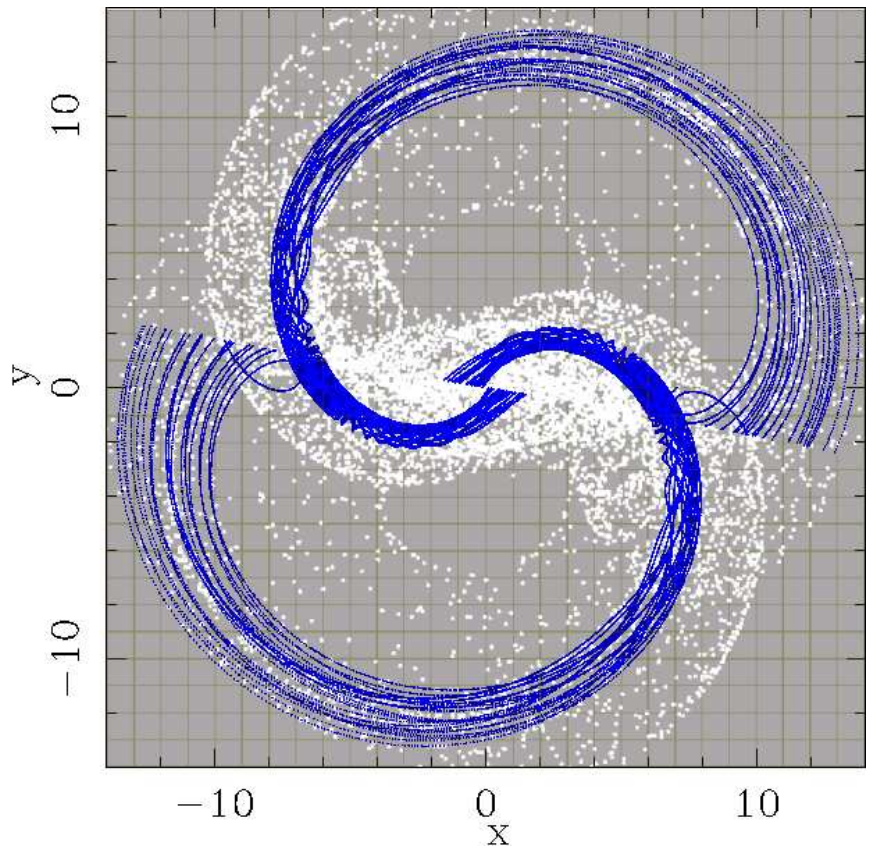

Photometrics: Radial profile

The density profile along a cut across the ring and spiral arms has the same properties as in observations.
Romero-Gómez et al. (2006)

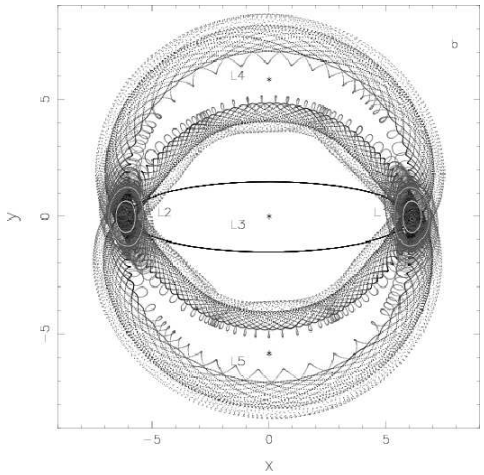

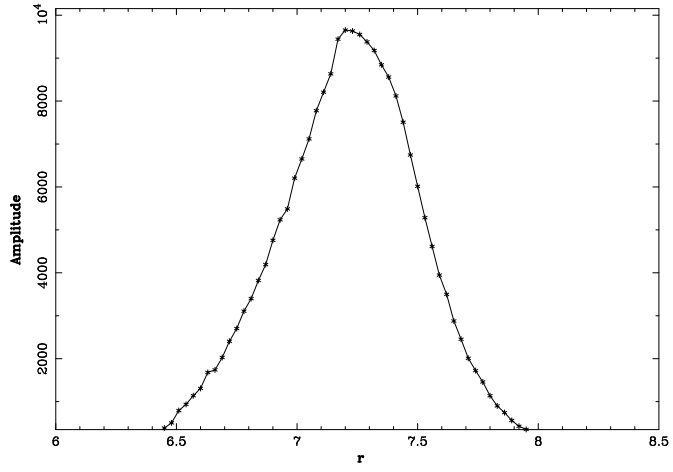

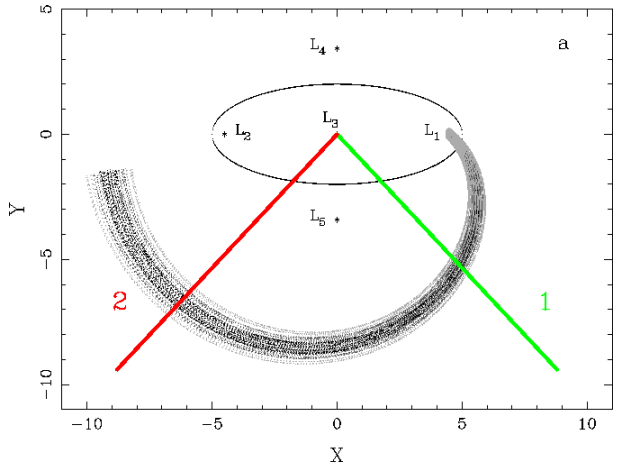

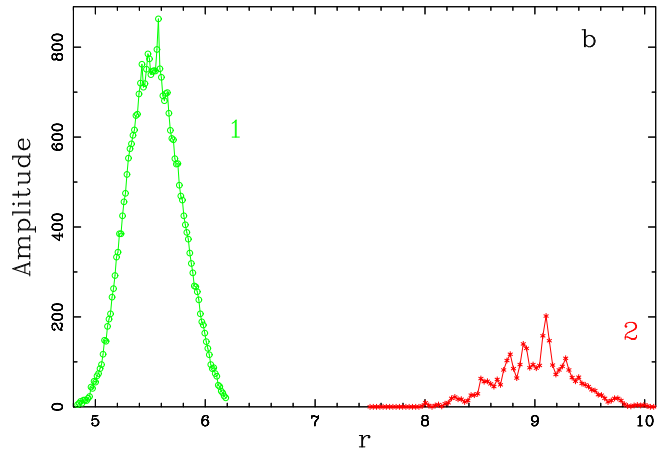

2D parameter study - BW type of bar

Athanassoula, Romero-Gómez & Masdemont (2008)

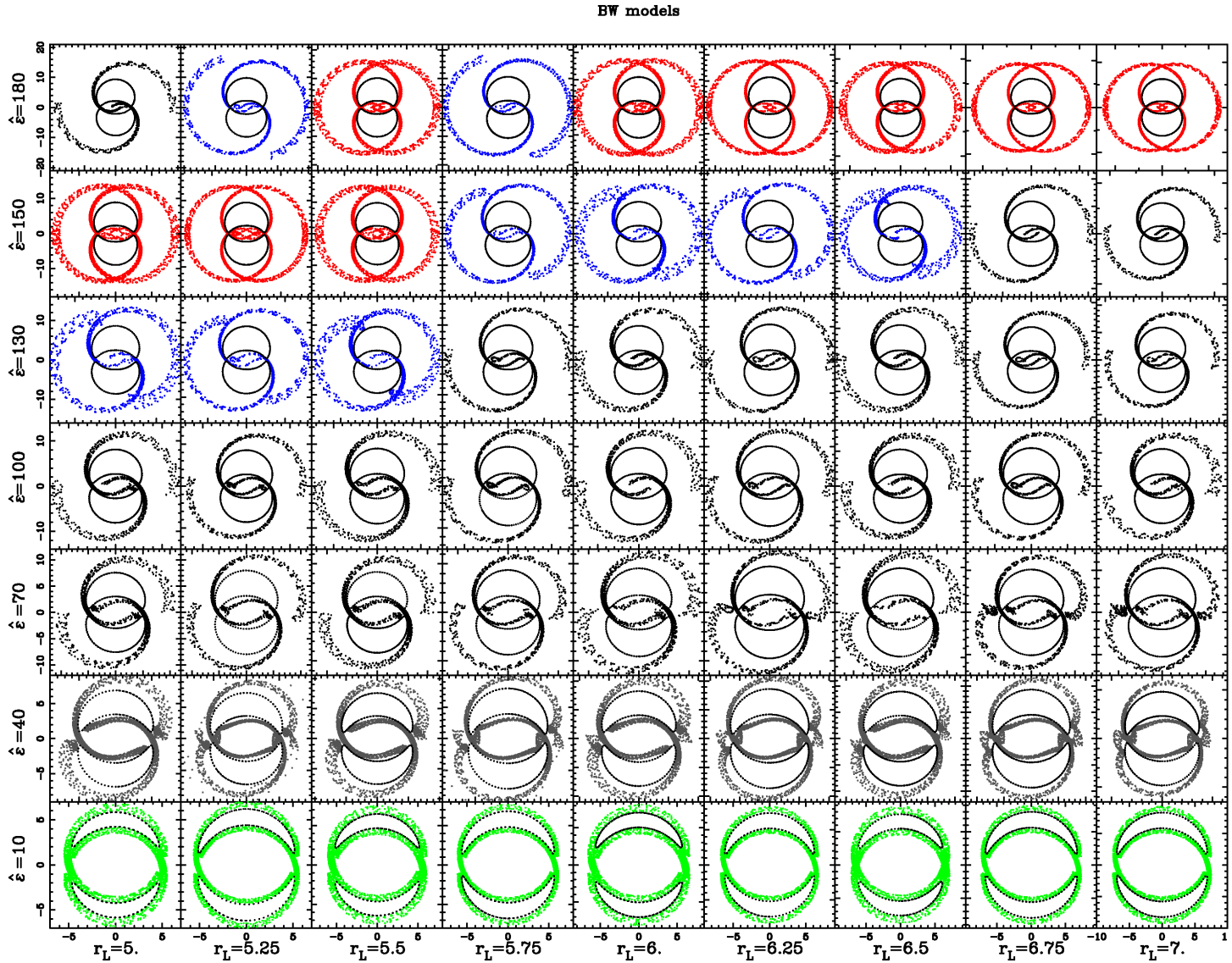

Is there a quantity, valid for all barred galaxy potentials, that can predict whether a model/galaxy will be spiral, R_1, R_2 or R_1R_2 ? Yes (?)

- $q_r = \dfrac{\partial\Phi_2/\partial r}{\partial\Phi_0/\partial r}$
- $q_t = \dfrac{(\partial\Phi/\partial\theta)_{max}}{r\partial\Phi_0/\partial r}$
- $\Phi_{\text{eff}} = \Phi - \frac{1}{2}\Omega_p^2\,(x^2+y^2)$
- $\text{RAT}=\dfrac{y_2}{y_1}$

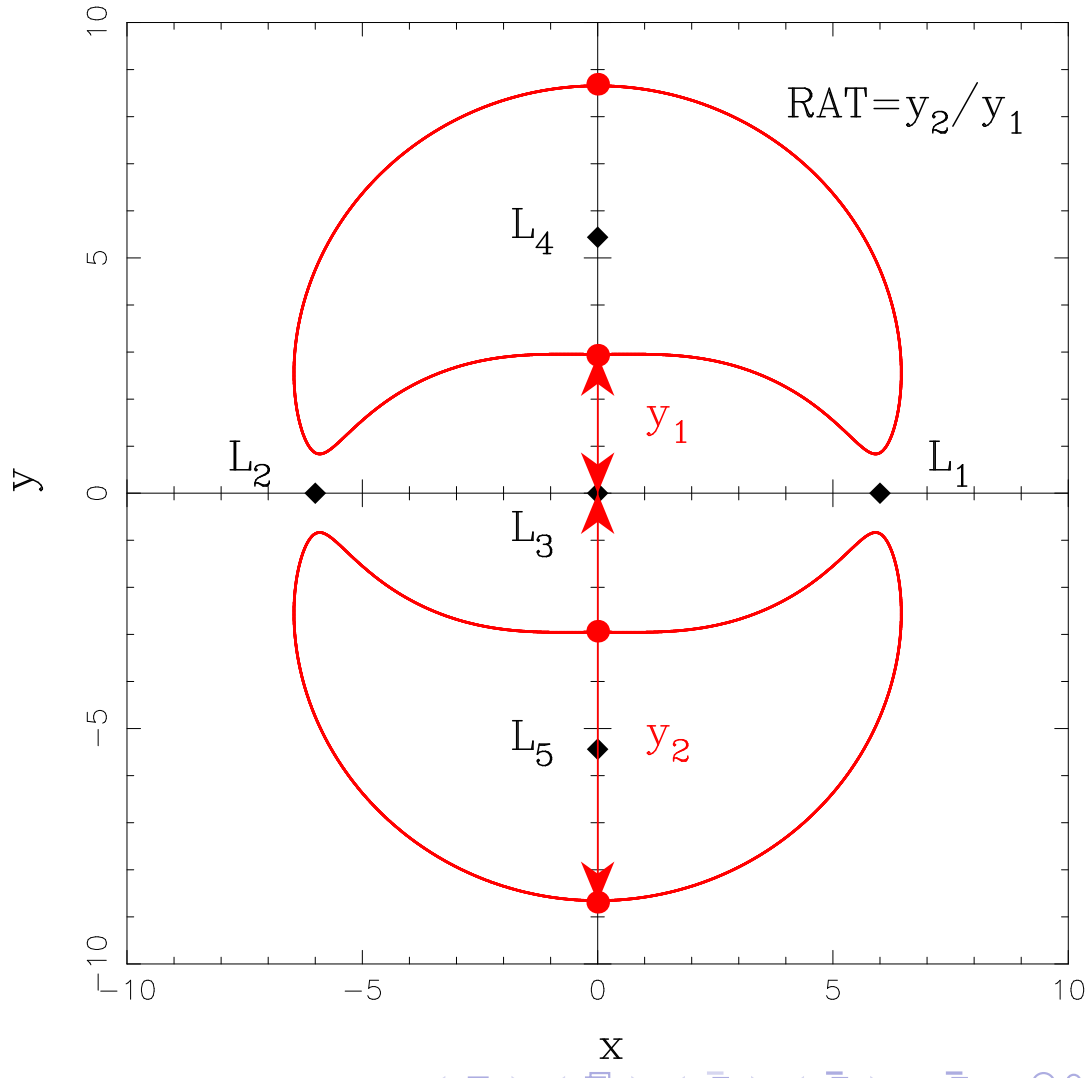

2D parameter study - prediction tool

Athanassoula, Romero-Gómez & Masdemont (2008)

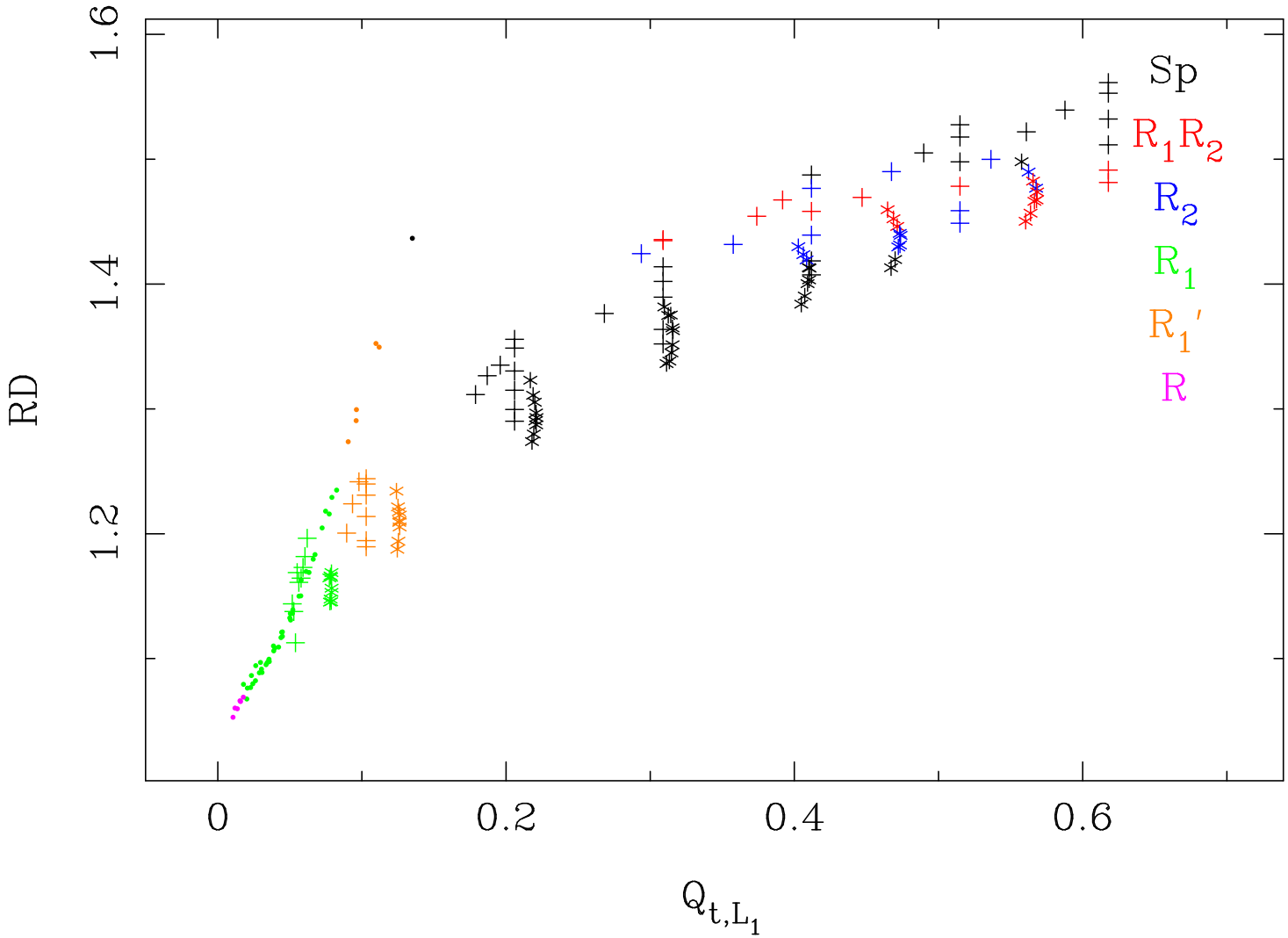

Pitch angle vs strength parameter

According to observations, the pitch angle of the spiral arm increases in galaxies with a strong bar.

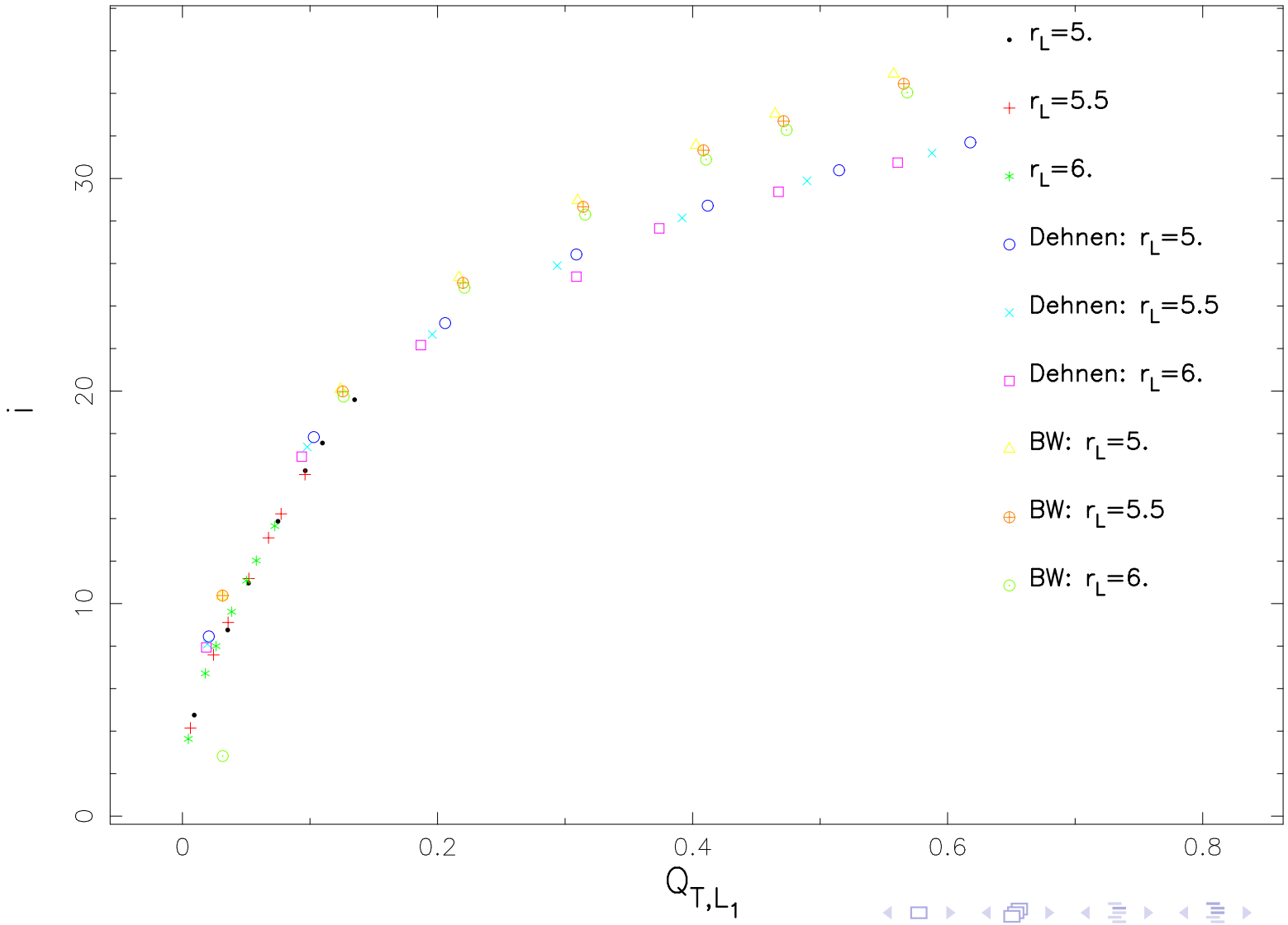

Photometrics: Pitch angle

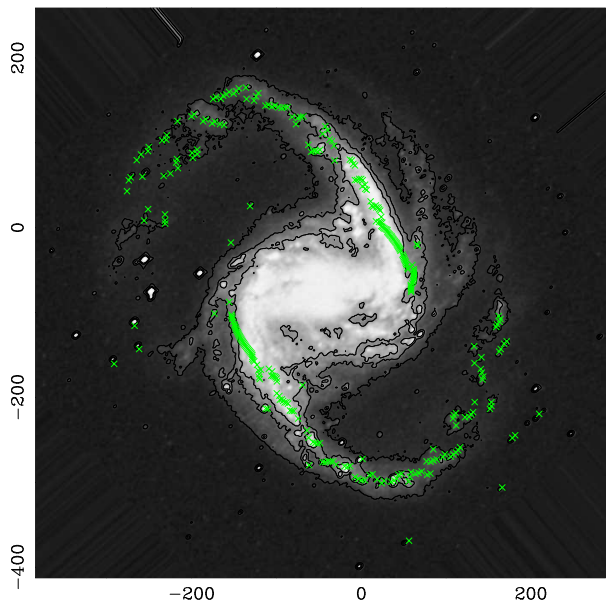

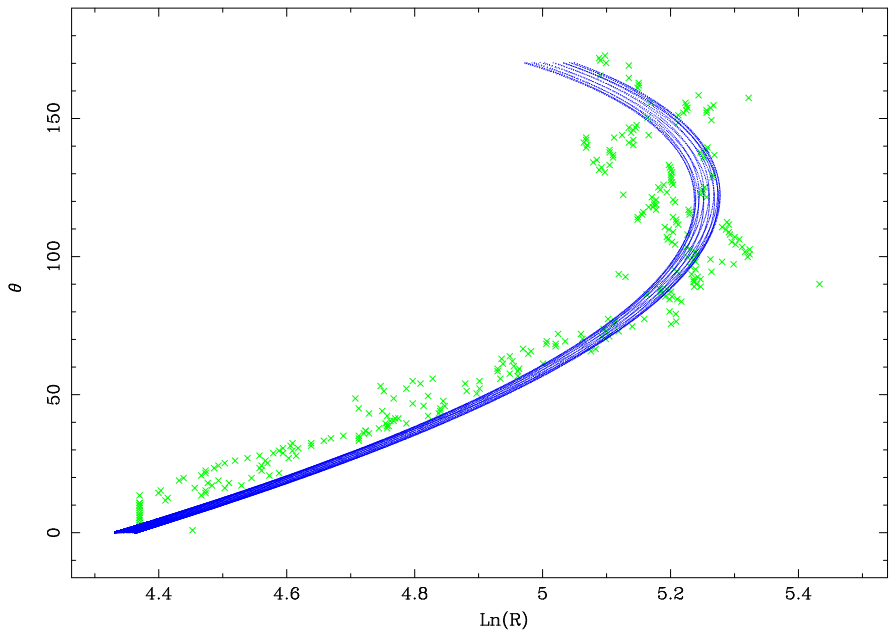

Ratio of the outer ring diameters vs strength parameter

We find a good correlation between the ratio of the outer ring diameters with the strength of the bar.

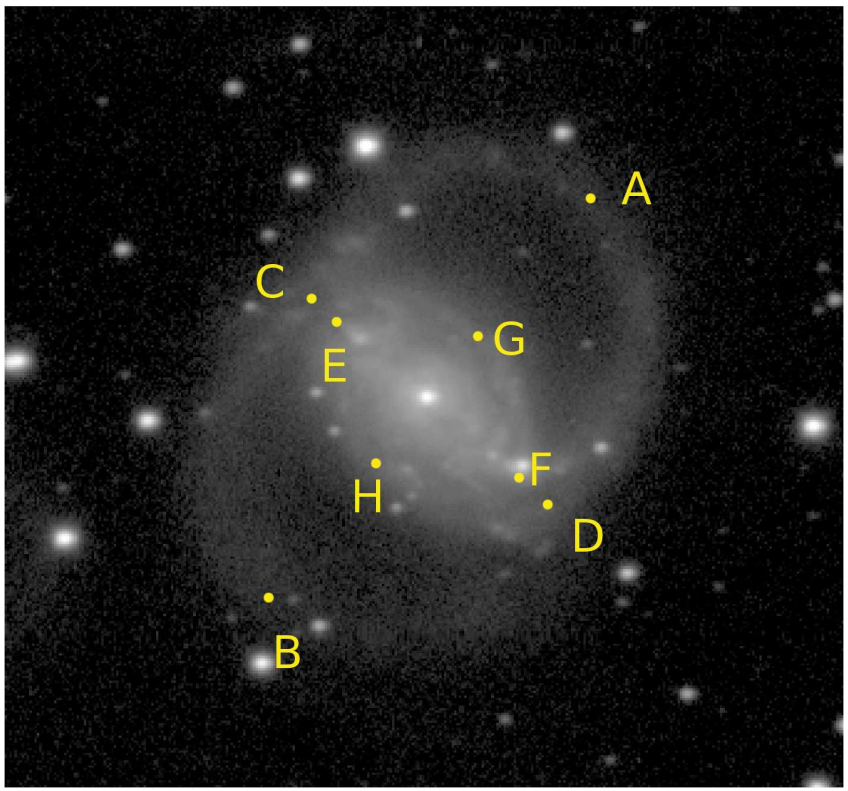

$$d_o/D_o = CD/AB$$

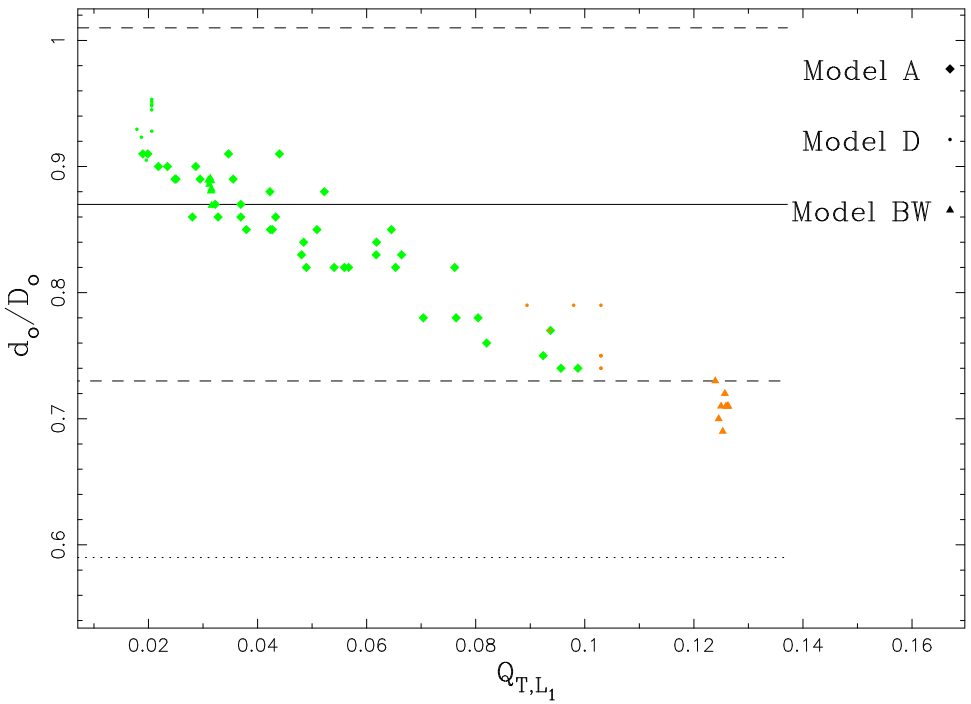

Stabilisation of L_1 and L_2 - ansae formation? -I

What if material gets concentrated at the ends of the bar?

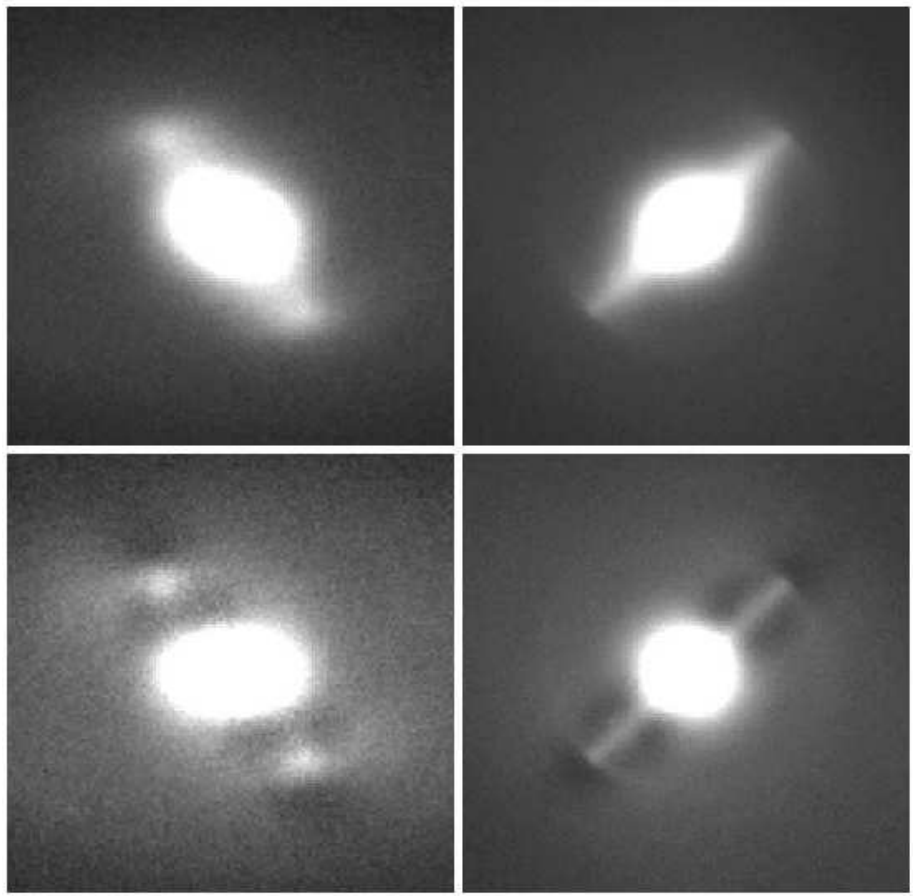

ansae bars "normal" bars

Stabilisation of L_1 and L_2 - ansae formation? -II

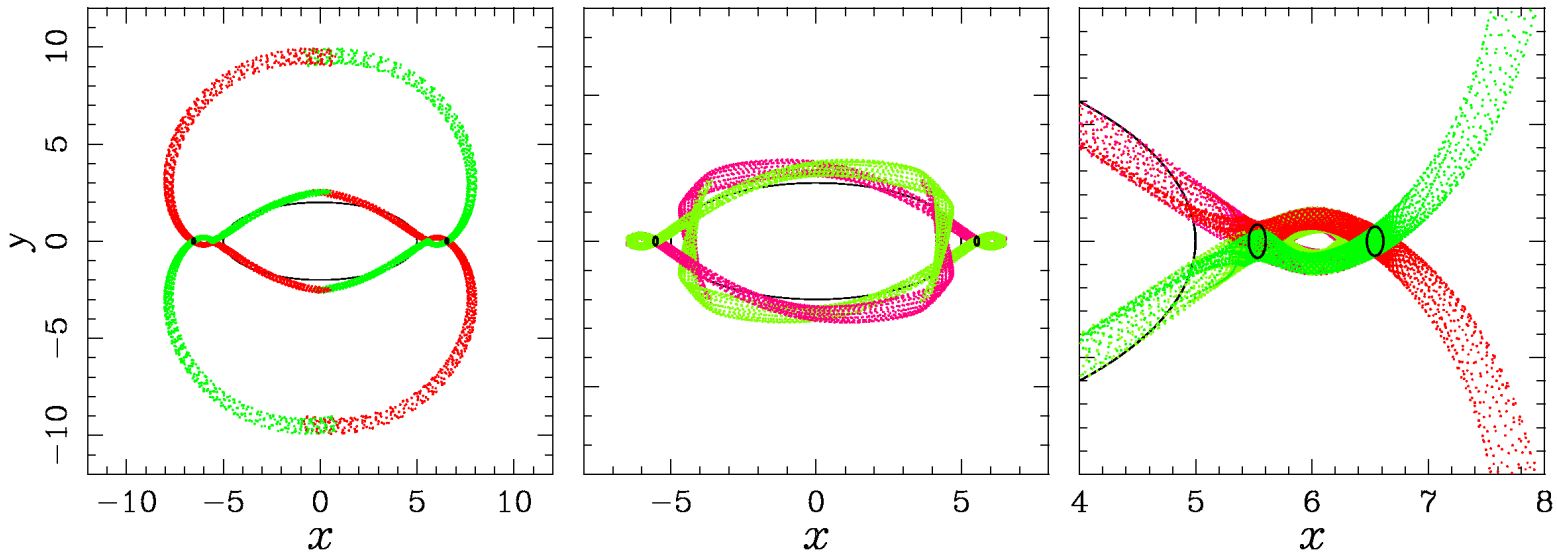

Thanks!

The Starry night (Vincent van Gogh)